for MAG. MAG binds directly to NgR, and NgR is necessary and sufficient for MAG inhibition of neurite outgrowth. Indeed, NgR expression in vivo is correlated with neuronal sensitivity to MAG, and the NgR protein is juxtaposed to compact myelin–containing MAG and Nogo (*20*). Thus, NgR must be considered a general receptor for restrictive effects of CNS myelin on axon growth in the adult mammalian CNS (Fig. 4C). Although MAG and Nogo-66 both bind to the LRRs of NgR, they appear to bind independently. This provides an explanation for similar but additive effects of Nogo and MAG on inhibition of axon growth. Evidence indicates that the NgR ligands, Nogo and MAG, are the two primary inhibitors in CNS myelin. Myelin prepared from mice lacking Nogo-A exhibits reduced inhibition of axon outgrowth, and the residual inhibitory activity is abolished by antibodies to MAG (*22*). Because one receptor mediates the action of both known myelin-derived inhibitors, interference with NgR function after CNS axonal injury may significantly alleviate myelin-dependent limitation of axonal regeneration.

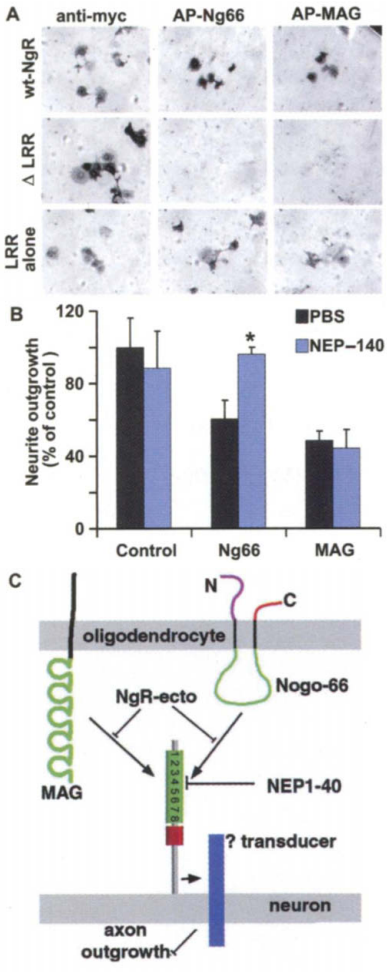

Fig. 4. Characterization of MAG binding site on the Nogo receptor. (**A**) COS-7 cells expressing full-length NgR (wtNgR), a NgR mutant lacking LRR 1-8 (ΔLRR), or a mutant containing LRR1-8 fused to the GPI linkage site (LRR alone) were stained for Myc immunoreactivity or tested for AP-Nogo-66 and AP-MAG binding. MAG and Nogo bind only to wtNgR and LRR alone transfected COS-7 cells. (**B**) NEP1-40 blocks Nogo-66 inhibitory activity but not that of MAG. Quantification of neurite outgrowth from dissociated E13 chick DRG cultures grown for 5 to 7 hours on PBS or MAG spots in the presence or absence of 1 μM NEP1-40. Means ± SEM of three experiments are reported. All $^*P$ values ≤ 0.002 (student's t test). (**C**) Model of NgR-mediated signaling. Either MAG or Nogo-66 can activate NgR. These interactions are blocked by the presence of a dominant-negative NgR protein, NgR-Ecto. The peptide antagonist, NEP1-40, specifically inhibits Nogo-66 activity but not that of MAG. Interaction of the axonal NgR with either one of its ligands on oligodendrocytes is predicted to activate a transmembrane signal transducer to inhibit axon outgrowth.

References and Notes

1. J. Qiu, D. Cai, M. T. Filbin, *Glia* **29**, 166 (2000).
2. A. E. Fournier, S. M. Strittmatter, *Curr. Opin. Neurobiol.* **11**, 89 (2001).
3. M. T. Filbin, *Curr. Biol.* **10**, R100 (2000).
4. L. McKerracher, *Neurobiol. Dis.* **8**, 11 (2001).
5. A. B. Huber, M. E. Schwab, *Biol. Chem.* **381**, 407 (2000).
6. P. A. Brittis, J. G. Flanagan, *Neuron* **30**, 11 (2001).
7. A. E. Fournier, T. GrandPre, S. M. Strittmatter, *Nature* **409**, 341 (2001).
8. B. E. Collins *et al.*, *J. Biol. Chem.* **274**, 37637 (1999).
9. S. Tang *et al.*, *J. Cell Biol.* **138**, 1355 (1997).
10. L. J. Yang *et al.*, *Proc. Natl. Acad. Sci. U.S.A.* **93**, 814 (1996).
11. M. Vinson *et al.*, *J. Biol. Chem.* **276**, 20280 (2001).
12. S. Kelm *et al.*, *Curr. Biol.* **4**, 965 (1994).
13. B. E. Collins *et al.*, *J. Biol. Chem.* **272**, 16889 (1997).
14. N. Sawada, H. Ishida, B. E. Collins, R. L. Schnaar, M. Kiso, *Carbohydr. Res.* **316**, 1 (1999).
15. B. P. Liu, S. M. Strittmatter, unpublished data.
16. M. Li *et al.*, *J. Neurosci. Res.* **46**, 404 (1996).
17. A. Fournier, G. Gould, B. P. Liu, S. M. Strittmatter, unpublished data.
18. G. Mukhopadhyay, P. Doherty, F. S. Walsh, P. R. Crocker, M. T. Filbin, *Neuron* **13**, 757 (1994).
19. D. Cai *et al.*, *J. Neurosci.* **21**, 4731 (2001).
20. X. Wang *et al.*, *J. Neurosci.*, **22**, 5505 (2002).
21. T. GrandPre, S. Li, S. M. Strittmatter, *Nature* **417**, 547 (2002).
22. J. E. Kim, S. Li, T. GrandPre, D. Qiu, S. M. Strittmatter, unpublished data.

23. Supported by research grants from the NIH, the McKnight Foundation, the Institute for the Study of Aging, and Biogen, Inc. (S.M.S.); and an institutional training grant from the NIH (B.P.L.). T.G. is a Bayer predoctoral scholar, and S.M.S. is an investigator of the Patrick and Catherine Weldon Donaghue Medical Research Foundation.

Supporting Online Material

www.sciencemag.org/cgi/content/full/1073031/DC1
Materials and Methods

18 April 2002; accepted 13 June 2002
Published online 27 June 2002;
10.1126/science.1073031
Include this information when citing this paper.

Amphiphysin 2 (Bin1) and T-Tubule Biogenesis in Muscle

Eunkyung Lee,[1]* Melissa Marcucci,[1]* Laurie Daniell,[1] Marc Pypaert,[1] Ora A. Weisz,[2] Gian-Carlo Ochoa,[1] Khashayar Farsad,[1] Markus R. Wenk,[1] Pietro De Camilli[1]†

In striated muscle, the plasma membrane forms tubular invaginations (transverse tubules or T-tubules) that function in depolarization-contraction coupling. Caveolin-3 and amphiphysin were implicated in their biogenesis. Amphiphysin isoforms have a putative role in membrane deformation at endocytic sites. An isoform of amphiphysin 2 concentrated at T-tubules induced tubular plasma membrane invaginations when expressed in non-muscle cells. This property required exon 10, a phosphoinositide-binding module. In developing myotubes, amphiphysin 2 and caveolin-3 segregated in tubular and vesicular portions of the T-tubule system, respectively. These findings support a role of the bilayer-deforming properties of amphiphysin at T-tubules and, more generally, a physiological role of amphiphysin in membrane deformation.

Ultrastructural observations have suggested that T-tubules of striated muscle develop from beaded tubular invaginations of the plasma membrane that resemble strings of caveolae (*1*, *2*). Accordingly, recent studies have demonstrated a critical role for caveolin-3 in T-tubule biogenesis (*3*–*5*) and have implicated caveolin-3 in a form of human muscular dystrophy (*6*). However, the smooth tubular profile of the T-tubule system of mature muscles indicates that the function of caveolin is, at least in part, replaced by other proteins during muscle differentiation. In addition, T-tubules, albeit with an abnormal morphology, are present in mice lacking caveolin-3 (*5*), indicating that other proteins participate in tubulogenesis.

It was reported that a splice variant of amphiphysin 2 is expressed at very high levels in adult striated muscle [muscle or M-amphiphysin 2, also referred to as Bin1 (*7*, *8*)] and is localized at T-tubules (*7*). Amphiphysin proteins function

as adaptors between the plasma membrane and submembranous cytosolic scaffolds (*9*). They contain a highly conserved NH_2-terminal region (BAR domain), a COOH-terminal SH3 domain, and a variable central region (Fig. 1A). In amphiphysin 1 and in the predominant neuronal isoform of amphiphysin 2 (neuronal or N-amphiphysin 2), the central region contains binding sites for clathrin and adaptor protein- 2 (AP-2), reflecting a role of these proteins in endocytosis (*10–12*). Such sites are not present in M-amphiphysin 2, which instead contains a unique exon (exon 10), just downstream of the BAR domain (*7, 8*). In vitro studies have shown that the BAR domain of amphiphysin binds and evaginates lipid membranes into narrow tubules (*13–15*) suggesting that M-amphiphysin 2 may generate membrane curvature in vivo and perhaps contribute to the biogenesis of T-tubules. Muscle T-tubule defects were detected in *Drosophila* that harbor mutations in its only amphiphysin gene (*15*).

To gain mechanistic insight into the properties of M-amphiphysin 2, we expressed green fluorescent protein (GFP)-tagged isoforms of amphiphysin 1 and 2 in Chinese hamster ovary (CHO) cells. In spite of the reported lipid-binding properties of amphiphysin in vitro (*13*), both amphiphysin 1 and N-amphiphysin 2 had, primarily, a diffuse cytosolic distribution. In contrast, M-amphiphysin 2 was highly concentrated at the cell surface (Fig. 1B). Plasma membrane targeting was mediated by the BAR domain and was dependent on exon 10 (Fig. 1). Exon 10 has a high basic amino acid content (9 out of 15, see Fig. 1A) and has an overall resemblance to phosphatidylinositol-4,5-bisphosphate [$PI(4,5)P_2$]–binding amino acid sequences (*16, 17*). Binding of the BAR domain to liposomes was enhanced by the presence of exon 10 when liposomes contained $PI(4,5)P_2$ [and to a lesser extent phosphatidylinositol-4-phosphate, PI(4)P] (Fig. 1C). Thus, the targeting of M-amphiphysin 2 to the plasma membrane is likely to be mediated by binding of its BAR domain, including exon 10 (BAR* domain), to PI(4)P and $PI(4,5)P_2$. This result is consistent with the selective enrichment of $PI(4,5)P_2$ in the plasma membrane (*17*).

Transfected CHO cells expressing full-length GFP-tagged M-amphiphysin 2 revealed an accumulation of numerous narrow tubular structures continuous with the plasma membrane as seen by electron microscopy (Fig. 2A) and by their accessibility to the membrane impermeable fluorescence dye FM4-64 (fig. S1A). Furthermore, a GFP-tagged pleckstrin homology domain of phospholipase Cδ ($PH_{PLC\delta}$), a protein module that binds $PI(4,5)P_2$ and thus acts as a plasma membrane marker (*17*), was targeted to these tubules when coexpressed with untagged M-amphiphysin 2 (fig. S1A). Incubation of recombinant M-amphiphysin 2 with liposomes caused their evagination into tubules similar in size to those found in transfected cells (Fig. 2C). These results indicate that the powerful liposome tubulating activity of amphiphysin observed in vitro (*13–15*) is a property that is relevant in vivo.

Dynamin 2, a binding partner of the SH3 domain of amphiphysin (*9*), was recruited to the tubules when coexpressed with M-amphiphysin 2 (Fig. 2D), but not when coexpressed with its BAR* domain, which was sufficient to induce tubulation (Fig. 2, B and E). Endogenous dynamin 2 was also partially recruited to the tubules by M-amphiphysin 2, but not by the

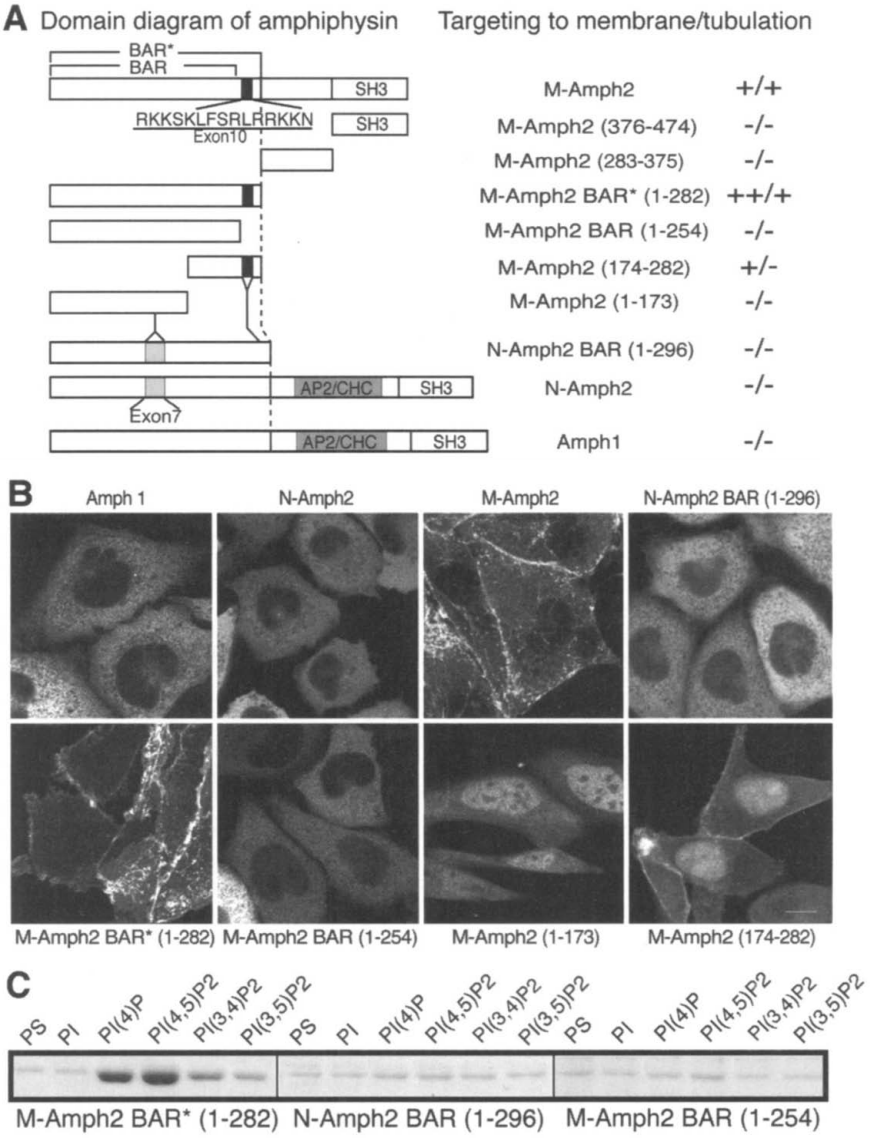

Fig. 1. Targeting of M-amphiphysin 2 to the plasma membrane mediated by the phosphoinositide-binding properties of exon 10. **(A)** Domain diagram of amphiphysin constructs tested by transfection of the corresponding GFP fusion proteins and summary of localization results. AP2/CHC marks the location of binding sites for the clathrin adaptor AP-2 and clathrin heavy chain. **(B)** GFP fluorescence of CHO cells expressing some of the constructs depicted in (A). Full-length M-amphiphysin 2 and its and BAR* domain are targeted to the plasma membrane and induce the appearance of linear elements (tubules). The second half of the BAR* domain, which contains exon 10 [M-Amph2 (174 to 282)], is targeted to the membrane, but does not induce these structures, in agreement with the previous mapping of the membrane tubulation property of the BAR domain to its NH_2-terminal portion (*14*). The two smallest fragments (bottom right panels) are also present in the nucleus, presumably due to their size. **(C)** Binding of the BAR* domain of M-amphiphysin 2 to PI(4)P and $PI(4,5)P_2$ via exon 10 as assessed by a liposome-binding assay. All BAR domains exhibit some liposome binding [see also (*13, 14*)], but enhanced binding to liposomes containing $PI(4,5)P_2$ and to a lesser extent PI(4)P was observed for the BAR* domain of M-Amphiphysin 2. Scale bar, 10 μm.

[1]Department of Cell Biology and Howard Hughes Medical Institute, Yale University School of Medicine, 295 Congress Avenue, New Haven, CT 06510, USA. [2]Renal-Electrolyte Division, University of Pittsburgh, 3550 Terrace Street, Pittsburgh, PA 15261, USA.

*These authors contributed equally to this work.
†To whom correspondence should be addressed. E-mail: pietro.decamilli@yale.edu

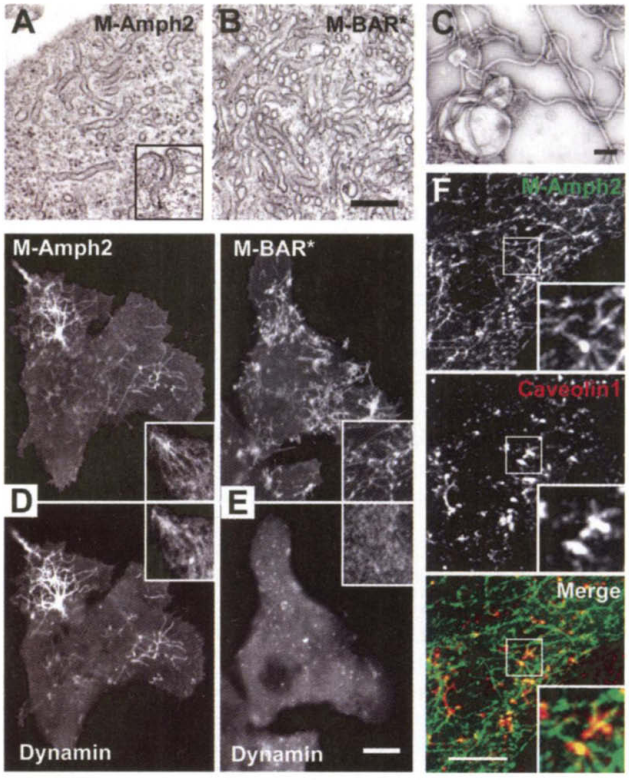

Fig. 2. In vivo and in vitro tubulation of lipid membranes by M-amphiphysin 2. (**A** and **B**) Electron microscopic views of transfected CHO cells expressing either M-amphiphysin 2 (A) or its BAR* domain (B) reveal the presence of narrow tubules continuous with the plasma membrane [inset of (A)]. (**C**) Electron micrograph demonstrating the massive tubulation of liposomes induced by recombinant M-amphiphysin 2. (**D** and **E**) GFP–dynamin 2 is recruited to tubules when coexpressed with untagged full-length M-amphiphysin 2 (D), but not when coexpressed with the BAR* domain, which lacks the SH3 domain (E). In these two fields, M-amphiphysin 2 and BAR* domain were detected by immunofluorescence. Insets of (D) and (E) show endogenous dynamin immunoreactivity in cells transfected with GFP–M-amphiphysin 2 full-length and GFP-BAR*, respectively. (**F**) Double immunofluorescence for caveolin-1 and amphiphysin of M-amphiphysin 2–transfected CHO cells. Caveolin-1 immunoreactivity (red) is detectable in a punctate pattern along M-amphiphysin 2–positive tubules (green). Scale bars, 200 nm in (A to C) and 20 μm in (F).

BAR* domain (insets of Fig. 2, D and E, respectively). Tubules induced by the BAR* domain alone were often closely opposed to each other (Fig. 2B), whereas those induced by full-length M-amphiphysin 2 were always separated by cytoplasmic matrix (Fig. 2A), possibly reflecting the presence of a protein scaffold including dynamin 2.

We investigated the temporal and spatial expression pattern of M-amphiphysin 2 during muscle differentiation using the C2C12 myoblastic cell line. Expression of amphiphysin 2 increased upon differentiation, as previously reported (*18*), and correlated with increased expression of caveolin (*3*–*5*) and the dihydropyridine receptor (DHPR) (*18*), a Ca^{2+} channel of T-tubules (*19*), and with the down-regulation of caveolin-1 (Fig. 3A). Immunofluorescence staining for M-amphiphysin 2 in differentiated C2C12 cells produced a staining pattern represented by linear elements reminiscent of those seen in M-amphiphysin 2–expressing fibroblasts (Fig. 3B). DHPR-immunoreactive puncta were aligned with these elements. Caveolin-3 immunostaining was often aligned with these tubules but in a discontinuous fashion (Fig. 3C). Electron microscopy of differentiated C2C12 myotubes after cytochemical staining of cell-surface membranes with either ruthenium red

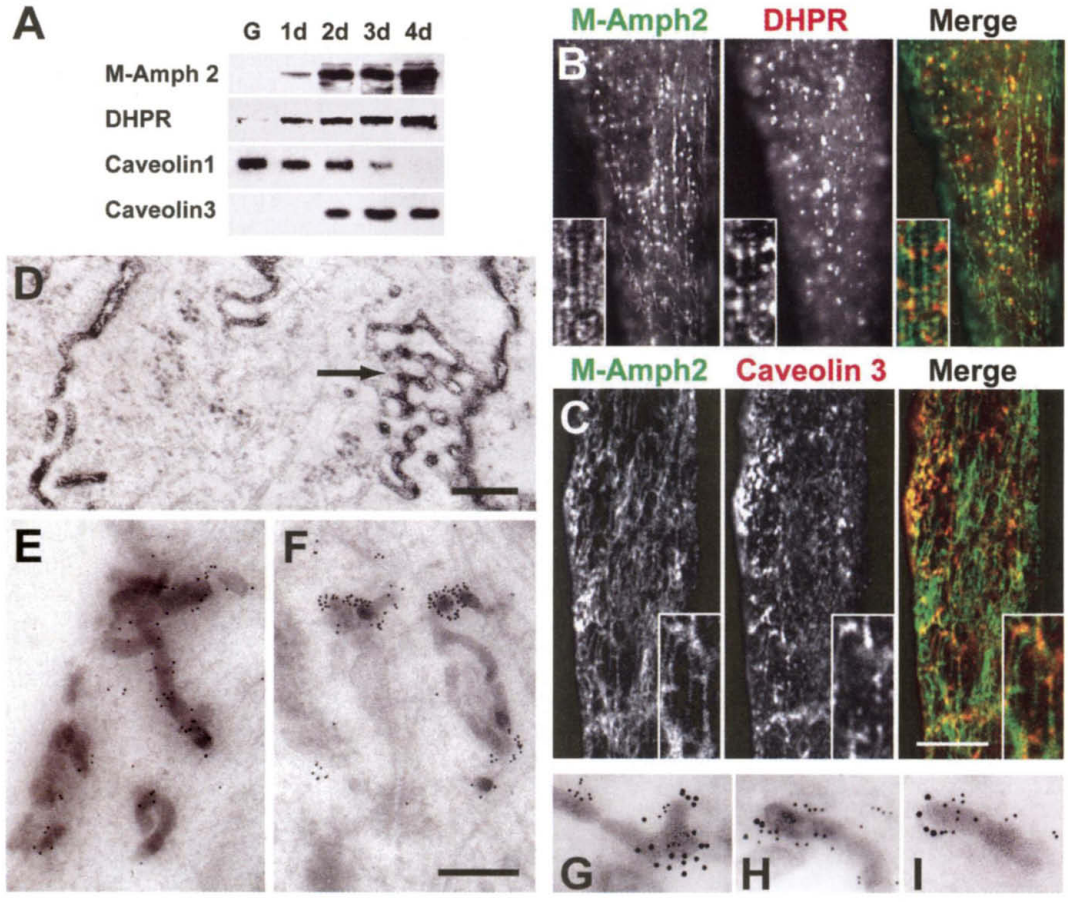

Fig. 3. Amphiphysin 2, DHPR, and caveolin in C2C12 cells. (**A**) Comparative analysis of the expression of amphiphysin 2, DHPR, caveolin-1, and caveolin-3, during cell differentiation. (**B** and **C**) Immunofluorescence microscopy of differentiated C2C12 myotubes demonstrating localization of endogenous amphiphysin 2 on tubular elements and partial overlap of amphiphysin 2 with DHPR and caveolin-3. The insets of (B) and (C) show that puncta of DHPR and caveolin-3 immunoreactivity are often aligned with amphiphysin 2–positive tubules. The images of (C) were obtained by confocal miscroscopy. (**D**) Electron micrograph of differentiated C2C12 myotubes after incubation with ruthenium red demonstrates the presence of deep, tubulovesicular plasma membrane invaginations (arrow). Localization of amphiphysin 2 (**E**) and caveolin-3 (**F**) in ultrathin frozen section of differentiated C2C12 myotubes as revealed by single immunogold labeling. (**G** to **I**) Samples prepared as in (E) and (F), but double-labeled for M-amphiphysin 2 (small gold) and caveolin-3 (large gold). In (E to I), amphiphysin 2 and caveolin-3 are concentrated on the tubular and vesicular portion, respectively, of the HRP-labeled network. Scale bars, 10 μm in (B) and (C); 200 nm in (D to I).

(*20*) (Fig. 3D) or horseradish peroxidase (HRP)–conjugated cholera toxin (*3*) revealed, as expected, a prominent network of surface-connected tubulovesicular structures (Fig. 3, E to I). Single (Fig. 3, E and F) and double (Fig. 3, G to I) immunogold labeling of ultrathin frozen sections of these cells revealed that the tubular portion of the network was intensely immunoreactive for amphiphysin 2, whereas caveolin-3 was preferentially concentrated on its vesicular domains. The segregation of caveolin-3 and amphiphysin 2 was amplified in adult skeletal muscle, where amphiphysin 2 was selectively localized on T-tubules, whereas caveolin-3 was primarily concentrated at the outer surface of the muscle fiber as previously reported (*6, 21*).

As M-amphiphysin 2–induced membrane tubules of transfected cells (fig. S1A), endogenous tubules of C2C12 cells accumulated GFP-$PH_{PLC\delta}$ (Fig. 4A), suggesting a high $PI(4,5)P_2$ content. If T-tubules are $PI(4,5)P_2$-positive, their massive proliferation during the differentiation of C2C12 cells should correlate with a major increase of $PI(4,5)P_2$ concentration in these cells. Indeed, the phosphoinositide content of differentiated C2C12 cells, as revealed by steady-state metabolic labeling with [^{3}H]*myo*-inositol, was increased by a factor of 10 over undifferentiated cells (Fig. 4B). The $PI(4,5)P_2$/PIP ratio was also increased to approximately 1.3 (SEM, 0.2), compared with 0.7 (SEM, 0.1) in undifferentiated cells (see also Fig. 4C). The concentration of $PI(4,5)P_2$ on T-tubules has important physiological implications for muscle contraction because $PI(4,5)P_2$ is the precursor of inositol trisphosphate (IP_3), a regulator of calcium signaling, and may also directly regulate T-tubule ion channels (*22*).

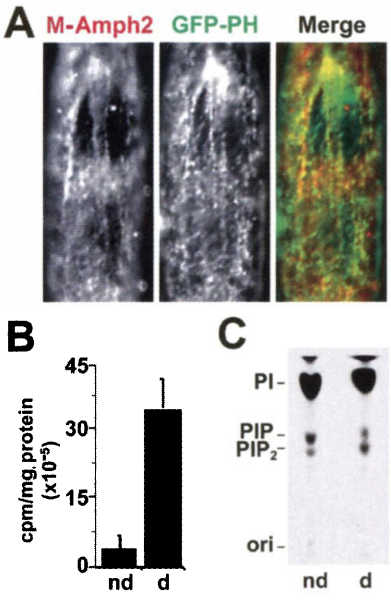

Fig. 4. $PI(4,5)P_2$ in differentiated C2C12 cells. (**A**) GFP-$PH_{PLC\delta}$–expressing cells were fixed and immunostained for M-amphiphysin 2. (**B**) Cells were metabolically labeled with [^{3}H]*myo*-inositol. The phosphoinositide content per milligram of protein of differentiated myotubes (d) is higher by a factor of 10, compared with undifferentiated cells (nd). (**C**) Equal amounts of radioactive lipids were separated by thin-layer chromatography. Note elevated levels of $PI(4,5)P_2$ and an increased ratio of PI(4,5)/PIP in differentiated C2C12 cells.

In agreement with the role of caveolin and caveolae in early stages of T-tubule biogenesis, cholesterol depletion by amphotericin B was shown to impair T-tubule formation in C2C12 cells (*23*). Accordingly, we found that exposure of C2C12 cells to either methyl β-cyclodextrin (*24*) or amphotericin B disrupted the pattern of amphiphysin 2 and caveolin-3 immunoreactivity [fig. S3 and (*21*)]. In view of these observations, we also examined the relationship between M-amphiphysin 2–induced tubules, caveolin-1 [the major isoform of caveolin in fibroblasts (*25*)], and cholesterol in transfected CHO cells expressing M-amphiphysin 2. As in the case of caveolin-3 immunoreactivity in C2C12 cells, caveolin-1 puncta were often aligned with M-amphiphysin 2 tubules (Fig. 2F). In addition, cyclodextrin-mediated cholesterol depletion led to a collapse of the tubules (fig. S2, A and B). These findings reveal additional similarities between plasma membrane invaginations induced by M-amphiphysin 2 in fibroblastic cells and bona fide muscle T-tubules. Collectively, our results indicate that expression in fibroblasts of a single protein, M-amphiphysin 2, is sufficient to induce a tubular network that shares some morphological and biochemical similarities with T-tubules of muscle.

To study more directly whether amphiphysin 2 is required for T-tubule development, we suppressed its expression by RNA interference (RNAi) (*26*). Two pairs of small interfering RNA or silencing RNA (siRNA) specific for amphiphysin 2 were transfected into C2C12 before their differentiation. Both pairs, either separately or together, almost completely blocked the expression of amphiphysin 2 and reduced the expression of caveolin-3 without affecting expression of dynamin 2 (fig. S4). More generally, they inhibited myoblast fusion and differentiation under these in vitro conditions [fig. S4B and (*21*)], which is consistent with results obtained by partial disruption of amphiphysin 2 expression by means of the antisense RNA technique (*18*). Although this effect of amphiphysin 2 suppression did not allow us to assess the role of M-amphiphysin 2 in the context of a mature myotube, it emphasized the important role of amphiphysin 2 in muscle differentiation.

The role of caveolin-3 in the biogenesis of T-tubules is complemented by amphiphysin during T-tubule maturation. Additional factors are likely to contribute to the morphology of mature T-tubules, because in amphiphysin *Drosophila* mutants the T-tubule system is abnormal but not absent (*15*). The results of this study provide evidence for a physiological function of the membrane-deforming properties of amphiphysin and for a role of alternative splicing in determining its sites of action. The clathrin- and AP-2–binding domains present in mammalian amphiphysin 1 and in N-amphiphysin 2, target amphiphysin to clathrin-coated pits, where amphiphysin may assist in the generation of a narrow tubular neck (*13*). Exon 10, instead, constitutively targets M-amphiphysin 2 to the plasma membrane, particularly to the cell compartment where the bulk of $PI(4,5)P_2$ is localized. The high concentration of M-amphiphysin 2 at the plasma membrane, in turn, results in massive tubular invagination. Thus, the BAR domain may be used in two different cellular contexts, but with similar roles in membrane morphogenesis. It will be of interest to determine the role of the SH3-mediated interactions of amphiphysin in T-tubule physiology.

References and Notes

1. H. Ishikawa, *J. Cell Biol.* **38**, 51 (1968).
2. S. Schiaffino, M. Cantini, S. Sartore, *Tissue Cell* **9**, 437 (1977).
3. R. G. Parton, M. Way, N. Zorzi, E. Stang, *J. Cell Biol.* **136**, 137 (1997).
4. E. M. McNally *et al.*, *Hum. Mol. Genet.* **7**, 871 (1998).
5. F. Galbiati *et al.*, *J. Biol. Chem.* **276**, 21425 (2001).
6. F. Galbiati, B. Razani, M. P. Lisanti, *Trends Mol. Med.* **7**, 435 (2001).
7. M. H. Butler *et al.*, *J. Cell Biol.* **137**, 1355 (1997).
8. R. Wechsler-Reya, D. Sakamuro, J. Zhang, J. Duhadaway, G. C. Prendergast, *J. Biol. Chem.* **272**, 31453 (1997).
9. V. I. Slepnev, P. De Camilli, *Nature Rev. Neurosci.* **1**, 161 (2000).
10. H. T. McMahon, P. Wigge, C. Smith, *FEBS Lett.* **413**, 319 (1997).
11. A. R. Ramjaun, K. D. Micheva, I. Bouchelet, P. S. McPherson, *J. Biol. Chem.* **272**, 16700 (1997).
12. V. I. Slepnev, G. C. Ochoa, M. H. Butler, P. De Camilli, *J. Biol. Chem.* **275**, 17583 (2000).
13. K. Takei, V. I. Slepnev, V. Haucke, P. De Camilli, *Nature Cell Biol.* **1**, 33 (1999).
14. K. Farsad *et al.*, *J. Cell Biol.* **155**, 193 (2001).
15. A. Razzaq *et al.*, *Genes Dev.* **15**, 2967 (2001).
16. T. F. Martin, *Annu. Rev. Cell Dev. Biol.* **14**, 231 (1998).
17. P. Varnai, T. Balla, *J. Cell Biol.* **143**, 501 (1998).
18. R. J. Wechsler-Reya, K. J. Elliott, G. C. Prendergast, *Mol. Cell. Biol.* **18**, 566 (1998).
19. A. H. Sharp, T. Imagawa, A. T. Leung, K. P. Campbell, *J. Biol. Chem.* **262**, 12309 (1987).
20. H. Damke, T. Baba, D. E. Warnock, S. L. Schmid, *J. Cell Biol.* **127**, 915 (1994).
21. E. Lee *et al.*, unpublished observations.
22. D. W. Hilgemann, S. Feng, C. Nasuhoglu, *Sci. STKE* (2001), http://stke.sciencemag.org/cgi/content/full/sigtrans;2001/111/re19.
23. A. J. Carozzi, E. Ikonen, M. R. Lindsay, R. G. Parton, *Traffic* **1**, 326 (2000).
24. E. B. Neufeld *et al.*, *J. Biol. Chem.* **271**, 21604 (1996).
25. P. E. Scherer *et al.*, *J. Biol. Chem.* **272**, 29337 (1997).
26. S. M. Elbashir *et al.*, *Nature* **411**, 494 (2001).

27. We thank V. Slepnev (our laboratory), S. Ferro-Novick (Yale University, CT), A. De Matteis (Mario Negr: Sud, Italy), and K. Campbell (University of Iowa, IA) for the generous gift of reagents. We also thank K. Cohen for her technical assistance. This work was supported by grants from the National Institutes of Health (NS36251 and CA46128 to P.D.C). E.L. is an American Cancer Society fellow.

Supporting Online Material

www.sciencemag.orgcgi/content/full/297/5584/1193/DC1
Materials and Methods
Figs. S1 to S4

27 February 2002; accepted 12 July 2002